

$\text{Ln}_2(\text{OH})_4\text{SO}_4 \cdot n\text{H}_2\text{O}$ (Ln = Pr to Tb; $n \sim 2$): A New Family of Layered Rare-Earth Hydroxides Rigidly Pillared by Sulfate Ions

Jianbo Liang, Renzhi Ma, Fengxia Geng, Yasuo Ebina, and Takayoshi Sasaki*

International Center for Materials Nanoarchitectonics (MANA), National Institute for Materials Science (NIMS), 1-1 Namiki, Tsukuba, Ibaraki, 305-0044, Japan

Received August 6, 2010

A new family of layered rare-earth hydroxides rigidly pillared by sulfate ions has been synthesized through homogeneous precipitation of lanthanide sulfate salts driven by hydrolysis of hexamethylenetetramine. Obtained materials were composed of aggregated thin platelet microcrystallites. Chemical analysis indicates that these samples have a general chemical formula of $\text{Ln}_2(\text{OH})_4\text{SO}_4 \cdot n\text{H}_2\text{O}$ (Ln = Pr to Tb; $n \sim 2$). The compounds are crystallized in an *A*-base-centered orthorhombic structure with unit cell dimensions of $a \sim 0.63$ nm, $b \sim 1.6$ – 1.7 nm, and $c \sim 0.37$ nm. Fourier transform infrared (FT-IR) spectra indicate that sulfate ions are in a *trans*-bidentate arrangement, which suggests that sulfate ions bridge adjacent rare-earth hydroxide layers through direct coordination to lanthanide cations. The compounds showed two-step weight loss (200–275 °C and ~ 350 °C) in the heating process, which can be ascribed to dehydration and dehydroxylation, respectively. Robust lanthanide–sulfate chelate bondings can be inherited even after calcination above 450 °C to yield layered oxysulfates of $\text{Ln}_2\text{O}_2\text{SO}_4$. Trends in compositional and structural features as well as bonding aspects of hydroxyl groups and sulfate ions across the series, Pr to Tb, are described. Eu and Tb samples exhibited photoluminescence (PL) properties with characteristic red and green emissions, respectively, through both the direct excitation of lanthanide ions themselves and the charge-transfer channels between lanthanide ions and surrounding oxygen atoms.

Layered rare-earth hydroxides (LREHs), which have a general chemical formula of $\text{Ln}_2(\text{OH})_{6-m}(\text{A}^{x-})_{m/x} \cdot n\text{H}_2\text{O}$ (Ln: trivalent rare-earth ions; A: guest anions; $0.5 \leq m \leq 2.0$), represent an interesting class of host–guest compounds composed of cationic lanthanide hydroxide layers and guest anions.^{1–8} Recently, LREHs have attracted increasing attention because their intercalation properties

and the unique physicochemical functions of lanthanide elements offer new opportunities for designing novel functional materials.^{4,5,7,8} Intercalation chemistry of layered compounds is primarily dependent on the intrinsic host structure. In this respect, there are two major LREH series based on chemical composition and structural characteristics. The first series has a typical formula of $\text{Ln}_2(\text{OH})_5(\text{A}^{x-})_{1/x} \cdot n\text{H}_2\text{O}$ ($m = 1$), in which lanthanide cations are solely coordinated by hydroxyl groups and water molecules with a variable coordination number between eight and nine to produce positively charged lanthanide hydroxide layers. Interlayer guest anions are electrostatically bound to the host layers, facilitating anion exchangeability for the compounds comparable to that of well-known layered double hydroxides (LDHs).^{3–6} In contrast, in the second series, $\text{Ln}_2(\text{OH})_4(\text{A}^{x-})_{2/x} \cdot n\text{H}_2\text{O}$ ($m = 2$), the total coordination number of lanthanide cations is usually fixed at nine, and guest anions tend to coordinate to lanthanide cations rather than being freely accommodated in the gallery, a feature similar to that of layered hydroxy salts (LHSs).^{1–3} Accordingly, harsh reaction conditions are required for anion exchange of the latter series.²

Over the last several years, intensive efforts have been made to synthesize LREH compounds, mainly utilizing hydrothermal reaction or homogeneous precipitation, but the varieties are still limited in halide,^{1,5a,5b,6b} nitrate,^{2,3,5c,6a} and some special organic species (2,6-anthraquinonedisulfonate; 2,6-naphthalenedisulfonate).⁴ To grasp the

- (1) (a) Louër, D.; Louër, M. *J. Solid State Chem.* **1987**, *68*, 292. (b) Louër, D.; Louër, M.; Delgado, A. L.; Martinez, O. G. *Eur. J. Solid State Inorg. Chem.* **1989**, *26*, 241. (c) Lundberg, M.; Skarnulis, A. J. *Acta Crystallogr., Sect. B* **1976**, *32*, 2944. (d) Mullica, D. F.; Sappenfield, E. L.; Grossie, D. A. *J. Solid State Chem.* **1986**, *63*, 231.
- (2) Newman, S. P.; Jones, W. J. *Solid State Chem.* **1999**, *148*, 26.
- (3) (a) Haschke, J. M. *Inorg. Chem.* **1974**, *13*, 1812. (b) Holcombe, C. E. *J. Am. Ceram. Soc.* **1978**, *61*, 481. (c) Schildermans, I.; Mullens, J.; Yperman, J.; Franco, D.; van Poucke, L. C. *Thermochim. Acta* **1994**, *231*, 185.
- (4) Gándara, F.; Perles, J.; Snejkó, N.; Iglesias, M.; Gómez-Lor, B.; Gutiérrez-Puebla, E.; Monge, M. A. *Angew. Chem., Int. Ed.* **2006**, *45*, 7998.
- (5) (a) Geng, F.; Xin, H.; Matsushita, Y.; Ma, R.; Tanaka, M.; Izumi, F.; Iyi, N.; Sasaki, T. *Chem.–Eur. J.* **2008**, *14*, 9255. (b) Geng, F.; Matsushita, Y.; Ma, R.; Xin, H.; Tanaka, M.; Izumi, F.; Iyi, N.; Sasaki, T. *J. Am. Chem. Soc.* **2008**, *130*, 16344. (c) Geng, F.; Matsushita, Y.; Ma, R.; Xin, H.; Tanaka, M.; Iyi, N.; Sasaki, T. *Inorg. Chem.* **2009**, *48*, 6724. (d) Geng, F.; Ma, R.; Sasaki, T. *Acc. Chem. Res.* **2010**, *43*, 1177.
- (6) (a) McIntyre, L. J.; Jackson, L. K.; Fogg, A. M. *Chem. Mater.* **2008**, *20*, 335. (b) Poudret, L.; Prior, T. J.; McIntyre, L. J.; Fogg, A. M. *Chem. Mater.* **2008**, *20*, 7447. (c) McIntyre, L. J.; Prior, T. J.; Fogg, A. M. *Chem. Mater.* **2010**, *22*, 2635.
- (7) Lee, K.-H.; Byeon, S.-H. *Eur. J. Inorg. Chem.* **2009**, 929.
- (8) (a) Hu, L.; Ma, R.; Ozawa, T. C.; Sasaki, T. *Angew. Chem., Int. Ed.* **2009**, *48*, 3846. (b) Hu, L.; Ma, R.; Ozawa, T. C.; Sasaki, T. *Inorg. Chem.* **2010**, *49*, 2960. (c) Lee, B.-I.; Lee, K. S.; Lee, J. H.; Lee, I. S.; Byeon, S.-H. *Dalton Trans.* **2009**, 2490. (d) Hu, L.; Ma, R.; Ozawa, T. C.; Sasaki, T. *Chem.–Asian J.* **2010**, *5*, 248.

host–guest interaction in LREH compounds, it is essential to incorporate a wide variety of anions, especially those having anisotropic configuration as well as specific function, into the galleries to create new structures that may have novel properties. Sulfate groups, in T_d symmetry and with two negative charges, are known to promote various structural arrangements in layered inorganic solids. Representative examples are layered transition metal (typically Fe, Co, Ni, and Mn) hydroxysulfates, which have drawn considerable attention for their interesting magnetic properties, e.g., interlayer magnetic exchange through sulfate pillaring.⁹ As the sulfate groups have versatile functions, the present study explored new LREH compounds with sulfate as the guest anions.

In this paper, we report the synthesis and characterization of a new family of layered rare-earth hydroxides pillared by sulfate ions. Their structural features are discussed on the basis of Fourier transform infrared (FT–IR) spectra and thermal behavior as well as X-ray diffraction (XRD) data. The photoluminescence (PL) properties for Eu and Tb samples are also described.

Experimental Section

Materials. Rare-earth sulfates, $\text{Ln}_2(\text{SO}_4)_3 \cdot 8\text{H}_2\text{O}$ ($\text{Ln} = \text{Pr}$, Nd , Sm , Eu , Gd , and Tb) of 99.99% purity, were purchased from Aldrich. Na_2SO_4 and hexamethylenetetramine (HMT) of purity >99.5% were obtained from Wako Pure Chemical Co. These chemicals were used as received without further purification. Milli-Q filtered water with resistivity >18 $\text{M}\Omega \cdot \text{cm}$ was used throughout the experiments.

Synthesis. Reagents such as $\text{Ln}_2(\text{SO}_4)_3 \cdot 8\text{H}_2\text{O}$, Na_2SO_4 , and HMT were dissolved in 1 dm^3 of water to produce a concentration of 5, 25, and 1.8 mM, respectively, and the resulting solution was refluxed under nitrogen protection for 6 h. The precipitate formed was recovered by filtration, washed with copious amounts of water and ethanol in turns, and finally dried to a constant weight in a box with the relative humidity controlled at ~75%.

Chemical Analysis. The contents of rare-earth elements and sulfate ions were determined by inductively coupled plasma (ICP) atomic emission spectroscopy (Seiko SPS1700HVR) and ion chromatography (Toso LC-8020), respectively, after dissolving a weighed amount of sample in aqueous HCl solution. For determination of OH^- , a weighed sample (approximately 0.1 g) was dissolved in 25 cm^3 of standard HCl solution (0.1 M) and then back-titrated with standard NaOH solution (0.1 M) monitored by a pH meter. The pH value of the solution was plotted against the volume of NaOH solution added to identify the titration end point. Carbon and total hydrogen contents were estimated using a LECO CS-412 analyzer. Water content was calculated by subtracting the hydrogen amount in the hydroxyl group from the total hydrogen content.

Characterization. Powder XRD patterns were collected by a Rigaku Rint-2200 diffractometer with monochromatic Cu $K\alpha$ radiation ($\lambda = 0.15405 \text{ nm}$). Micrographs were obtained using a JEOL-1010 transmission electron microscope (TEM) at an

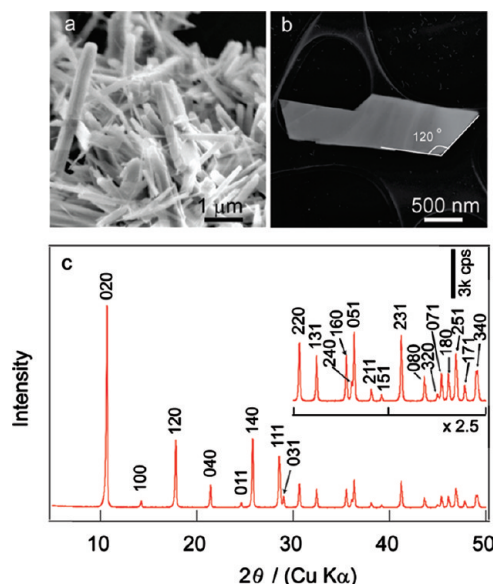


Figure 1. SEM and TEM images and XRD data of layered Tb-hydroxysulfate.

accelerating voltage of 100 kV. Specimens for TEM observation were prepared by dispersing the sample in ethanol with sonication followed by placing a droplet of dispersion on a holey carbon grid. The morphology and size of the samples were examined using a Keyence VE8800 scanning electron microscope (SEM). Fourier transform infrared (FT–IR) spectra were recorded using the KBr pellet method on a Varian 7000e FT–IR spectrophotometer equipped with a liquid-nitrogen-cooled MCT detector. Thermogravimetric differential thermal analysis (TG–DTA) measurement was carried out on a Rigaku TGA-8120 instrument in the temperature range of 25–1000 °C. Excitation and emission PL spectra were obtained at room temperature by means of a Hitachi F-4500 fluorescence spectrometer.

Results and Discussion

Synthesis and Characterization of Layered Tb-Hydroxysulfate. Refluxing a solution containing $\text{Tb}_2(\text{SO}_4)_3$, Na_2SO_4 , and HMT yielded a white precipitate. SEM and TEM observation of the recovered product revealed that it was composed of elongated platelets with edge length of up to several micrometers (Figure 1a,b). On the other hand, the platelet thickness was only tens of nanometers. Chemical analysis indicated that the composition of this sample was $\text{Tb}_{2.00}(\text{OH})_{4.02}(\text{SO}_4)_{0.99} \cdot 2.20\text{H}_2\text{O}$ (Anal. Calcd (%): Tb, 61.0; SO_4 , 18.2; OH, 13.1; H_2O , 7.6. Found (%): Tb, 60.4; SO_4 , 18.1; OH, 13.0; H_2O , 7.5). In addition, a tiny amount of carbon (0.1–0.2%) was detected. This may be attributable to a carbon residue from HMT decomposition, which is generally observed for hydroxides obtained via HMT hydrolysis. Accordingly, the chemical formula may be simplified as $\text{Tb}_2(\text{OH})_4\text{SO}_4 \cdot 2.2\text{H}_2\text{O}$. This chemical composition clearly indicates that the material obtained corresponds to the LREH series of $m = 2$.

The XRD pattern (Figure 1c) showed sharp diffraction peaks with d values of 0.830 and 0.415 nm in a low-angle region, being diagnostic of a layered structure. Nonbasal reflections were also sharp and symmetric even at a high-angle range, indicative of the highly crystalline nature of the

(9) (a) Vilminot, S.; Richard-Plouet, M.; André, G.; Swierczynski, D.; Bourée-Vigner, F.; Kurmoo, M. *Inorg. Chem.* **2003**, *42*, 6859. (b) Ben Salah, M.; Vilminot, S.; Richard-Plouet, M.; André, G.; Mhiri, T.; Kurmoo, M. *Chem. Commun.* **2004**, 2548. (c) Ben Salah, M.; Vilminot, S.; André, G.; Richard-Plouet, M.; Mhiri, T.; Takagi, S.; Kurmoo, M. *J. Am. Chem. Soc.* **2006**, *128*, 7972.

sample. All the diffraction peaks can be indexed on the basis of an orthorhombic structure with unit-cell parameters of $a = 0.62295(6)$, $b = 1.6581(1)$, and $c = 0.37040(4)$ nm. The stacking direction is parallel to the b -axis. Systematic absence of diffraction peaks of $k + l = 2n + 1$ for hkl indicates an A -base-centered symmetry, implying lateral gliding of adjacent layers with respect to each other and/or different orientation of sulfate ions. As a result, parameter b is double the basal spacing.

The obtained structural parameters show a close relationship to those for Tb-based hydroxides such as $\text{Tb}_2(\text{OH})_5\text{Cl} \cdot n\text{H}_2\text{O}^{5a,b}$ ($m = 1$ phase of LREH) and UCl_3 -type hexagonal $\text{Tb}(\text{OH})_3$.¹⁰ First, it should be noted that parameter a is close to the $\sqrt{3}$ times of c , suggesting that the host layer of the present compound has an ortho-hexagonal related architecture. In practice, frequently observed platelet morphology showing an angle of 120° at the platelet edge (Figure 1b) may be taken as evidence for this structural feature. Note that $\text{Tb}_2(\text{OH})_5\text{Cl} \cdot n\text{H}_2\text{O}$ has a similar pseudohexagonal sublattice and $\text{Tb}(\text{OH})_3$ is crystallized in the hexagonal system. In-plane parameter c of 0.37 nm, or the fundamental length of the present structure, is common for $\text{Tb}_2(\text{OH})_5\text{Cl} \cdot n\text{H}_2\text{O}$ and $\text{Tb}(\text{OH})_3$ structures, which are built up from the polyhedra of $\text{Tb}(\text{OH})_{8-\delta}(\text{H}_2\text{O})_\xi$ ($0 < \delta$, $\xi < 1$) and $\text{Tb}(\text{OH})_9$, respectively. The unique dimension of 0.37 nm for these compounds corresponds to the length between two neighboring edge-shared polyhedra or the nearest neighboring distance of Tb cations. On the basis of these structural considerations, we speculate that the host layer of the present Tb-hydroxysulfate compound is likely built up from Tb polyhedra as a fundamental structural unit. Tb ions may be coordinated to water molecules and sulfate ions as well as hydroxyl groups, and the resulting polyhedra are linked together into two-dimensional sheets with a pseudohexagonal architecture. This concept of structure is strengthened by the various characterization data presented below.

The FT-IR spectrum in Figure 2a provides some insight into the bonding aspects of hydroxyl groups and sulfate ions in the compound. Two sharp peaks at 3613 and 3477 cm^{-1} are assignable to the stretching modes of OH groups free from hydrogen bonding. The broad bands with two splitting peaks around 3261 and 3198 cm^{-1} are attributable to OH groups associated with hydrogen bonding. Peak broadening can be accounted for by interaction between hydroxyl groups and water molecules/gallery anions, which is commonly observed in LDH compounds as well as LREHs of $m = 1$ (Figure 2b).^{2,5} Other bands at around 1647, 812, and 594 cm^{-1} are due to the bending modes of water molecules coordinated to metal ions.¹¹ For sulfate ions, all the fundamental modes (ν_1 , ν_2 , ν_3 , and ν_4) can be observed in the spectrum. The appearance of ν_1 and ν_2 modes, IR inactive in the free sulfate ions of T_d point group, strongly suggests the lowering of site symmetry to C_{2v} . Notably, the ν_3 mode is split into three separate peaks,

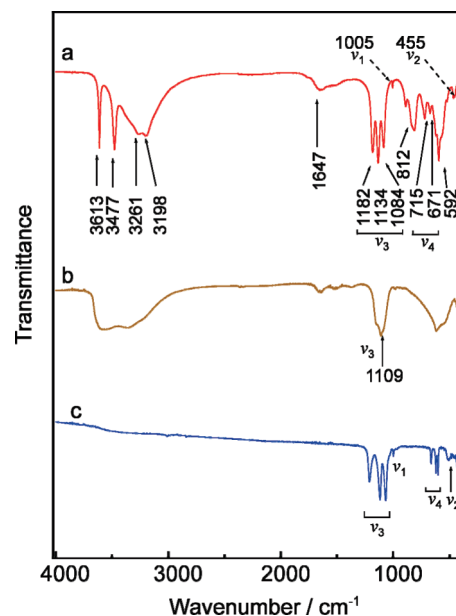


Figure 2. FT-IR spectrum of the samples: (a) layered Tb-hydroxysulfate, (b) sulfate-intercalated layered Tb hydroxide ($m = 1$ phase; $\text{Tb}_2(\text{OH})_5(\text{SO}_4)_{1/2} \cdot x\text{H}_2\text{O}$) derived from $\text{Tb}_2(\text{OH})_5\text{Cl} \cdot x\text{H}_2\text{O}$ through anion-exchange reaction and (c) layered $\text{Tb}_2\text{O}_2\text{SO}_4$ after calcination of layered Tb-hydroxysulfate at 1000°C .

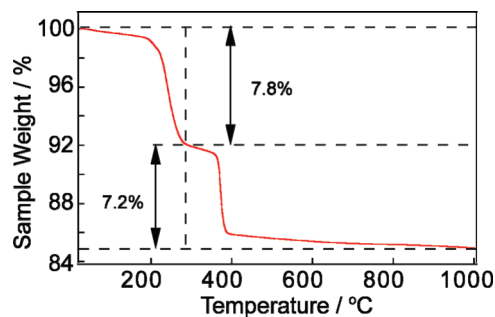


Figure 3. TG profile of layered Tb-hydroxysulfate.

very different from the broad single peak of the sulfate-intercalated layered Tb hydroxide (LREHs of $m = 1$; Figure 2b) as well as the corresponding LDHs. Such triple splitting of the ν_3 mode is characteristic of sulfate chelating as *trans*-bidentate ligands.¹¹ More importantly, these fundamental modes, especially the triple ν_3 mode, were observed in the spectrum even after calcination at 1000°C except for some shift of peaks (Figure 2c), indicating that sulfate ions in the compounds take a similar configuration after the heat treatment. The product after calcination is identified as $\text{Tb}_2\text{O}_2\text{SO}_4$ on the basis of XRD data, as will be described below. The structure of $\text{Tb}_2\text{O}_2\text{SO}_4$ can be described as alternating TbO_2^{2+} layers and sulfate groups, which bridge neighboring TbO_2^{2+} layers by directly coordinating to Tb^{3+} cations.^{12,13} These results evidently

(10) Beall, G. W.; Milligan, W. O.; Korp, J.; Bernal, I. *Acta Crystallogr., Sect. B* **1977**, *33*, 3134.

(11) Nakamoto, K. *Infrared and Raman Spectra of Inorganic and Coordination Compounds*, 4th ed.; Wiley: New York, 1986.

(12) (a) Machida, M.; Kawamura, K.; Ito, K. *Chem. Commun.* **2004**, 662. (b) Machida, M.; Kawamura, K.; Ito, K.; Ikeue, K. *Chem. Mater.* **2005**, *17*, 1487. (c) Machida, M.; Kawamura, K.; Kawano, T.; Zhang, D.; Ikeue, K. *J. Mater. Chem.* **2006**, *16*, 3084. (d) Machida, M.; Kawano, T.; Eto, M.; Zhang, D.; Ikeue, K. *Chem. Mater.* **2007**, *19*, 954.

(13) Zhukov, S.; Yatsenko, A.; Chernyshev, V.; Trunov, V.; Tserkovnaya, E.; Anston, O.; Höslä, J.; Baulés, P.; Schenk, H. *Mater. Res. Bull.* **1997**, *32*, 43.

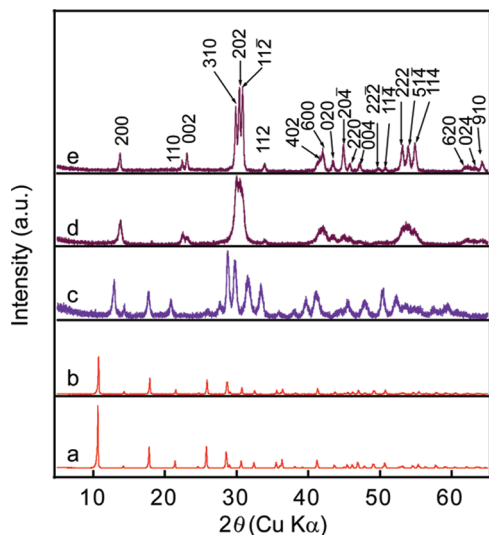


Figure 4. XRD patterns of (a) layered Tb-hydroxysulfate and products annealed at temperatures of (b) 150 °C; (c) 300 °C; (d) 450 °C; (e) 1000 °C.

indicate that sulfate groups in the present hydroxide compound are coordinated to Tb^{3+} cations. This is fully compatible with the structure model described above.

The compound lost weight in two separate steps upon heating, as depicted in Figure 3. The first weight loss of 7.8% in a temperature range of 200–275 °C is likely due to the removal of hydration water ($2.20 \text{ H}_2\text{O}$) in the chemical formula. In contrast to the related $m = 1$ phase of $\text{RE}_2(\text{OH})_5\text{A} \cdot x\text{H}_2\text{O}$ ($\text{A} = \text{Cl}$ and NO_3),^{5,6} dehydration took place sharply at a much higher temperature range, indicating that water molecules in the present hydroxysulfate are more strongly bound to the structure. Corresponding XRD data (Figure 4) indicate that the sample remained crystalline after dehydration although some degradation in crystallinity was observed. The subsequent weight loss took place again very sharply at ~ 350 °C, and this step can be attributed to dehydroxylation of the hydroxide layer. In fact, the observed weight loss of 7.2% is nearly equal to the expected value of 6.9% calculated from the chemical formula. The final product was identified as a single phase of $\text{Tb}_2\text{O}_2\text{SO}_4$, which was confirmed by the successful full indexing of the pattern based on previously reported data (JCPDS No. 41-0684). SEM images showed that $\text{Tb}_2\text{O}_2\text{SO}_4$ derived from the layered $\text{Tb}_2(\text{OH})_4\text{SO}_4 \cdot 2.2\text{H}_2\text{O}$ preserved the platelet morphology (Supporting Information, Figure S1).

Layered $\text{Ln}_2\text{O}_2\text{SO}_4$ has recently been reported as a useful material for large volume oxygen storage.¹² To date, layered $\text{Ln}_2\text{O}_2\text{SO}_4$ was synthesized by several methods including heating of $\text{Ln}_2(\text{SO}_4) \cdot 8\text{H}_2\text{O}$ salts,^{12a,b,14} thermal decomposition of DS-intercalated hydroxides,^{12c} or oxidation of Ln_2S_3 under controlled conditions.¹⁵ Nevertheless, the high processing temperature (over 800 °C) and release of SO_2 in these routes are neither economically nor envi-

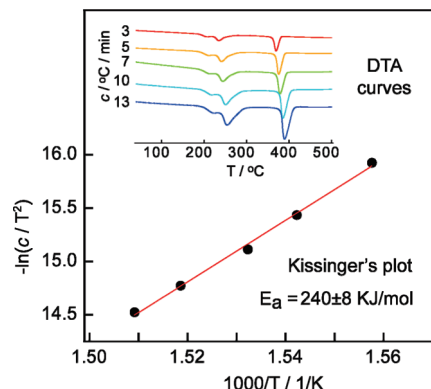
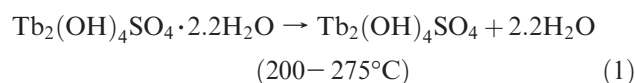


Figure 5. Kissinger's plot of dehydroxylation reaction of layered Tb-hydroxysulfate. T_m : temperature at DTA peak; c : heating rate. The inset shows DTA curves at various heating rates. See Supporting Information for details.

ronmentally desirable. The present results indicate that layered rare-earth hydroxysulfates containing stoichiometric sulfate, not only for the Tb form but also for other Pr–Eu samples (described in the following section), can be converted to layered $\text{Ln}_2\text{O}_2\text{SO}_4$ via the simple dehydroxylation reaction at 450 °C and above, which may be regarded as a convenient “green” route. This approach has obvious advantages for a lower annealing temperature in comparison with the processes reported previously.^{12,14}

The decomposition process of layered Tb-hydroxysulfate can be expressed as:



The kinetics of the dehydroxylation reaction (2) were studied by monitoring the transformation temperature as a function of the heating rate (Kissinger's approach¹⁶). The endothermic peaks associated with these processes shifted to a higher temperature with increasing heating rate. The apparent active energy (E_a), derived from Kissinger's plot ($-\ln(c/T_m^2)$ against $1000/T_m$ (c : heating rate; T_m : temperature at the DTA peak, Figure 5), is about $240 \pm 8 \text{ KJ/mol}$, nearly identical to that of $\text{La}(\text{OH})_3$ ($240 \pm 10 \text{ KJ/mol}$).¹⁷ This result suggests that hydroxyl groups in the layered Tb-hydroxysulfate are similar to those of the UCl_3 -type rare-earth hydroxides in both bonding and dehydroxylation kinetics.

On the basis of the structural characteristics disclosed, we propose a structure model for the layered Tb-hydroxysulfate compound as depicted in Figure 6: the $m = 2$ phase for $\text{Ln}_2(\text{OH})_{6-m}(\text{A}^{x-})_{m/x} \cdot n\text{H}_2\text{O}$. One Tb cation may be bonded to hydroxyl groups, water molecules, and oxygen atoms from the sulfate group to form a coordination polyhedron. The total coordination number should be nine. One hydroxyl group is shared by three

(14) (a) Hülising, H.; Kahle, H. G.; Kasten, A. *J. Magn. Magn. Mater.* **1980**, 15–18, 512. (b) Kahle, H. G.; Kasten, A. *J. Magn. Magn. Mater.* **1983**, 31–34, 1081. (c) Paul, W. *J. Magn. Magn. Mater.* **1990**, 87, 23.

(15) Yamamoto, S.; Tamura, S.; Imanaka, N. *J. Alloys Compd.* **2006**, 418, 226.

(16) Kissinger, H. E. *Anal. Chem.* **1957**, 29, 1702.

(17) Ozawa, M.; Onoe, R.; Kato, H. *J. Alloys Compd.* **2006**, 408–412, 556.

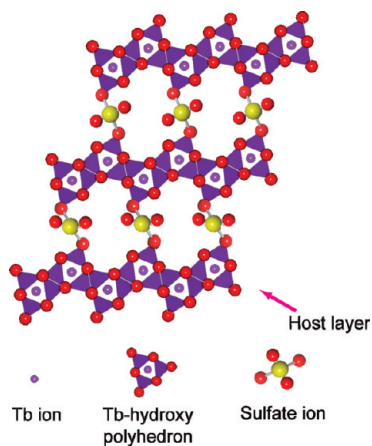


Figure 6. Plausible structure model for layered Tb-hydroxysulfate.

Table 1. Elemental Analysis Results on Layered Rare-Earth Hydroxysulfates

chemical formula		elemental analysis (%)			
		RE ³⁺	SO ₄ ²⁻	OH ⁻	H ₂ O
Pr _{2.00} (OH) _{3.98} (SO ₄) _{1.01} ·2.16H ₂ O	obsd.	57.8	19.8	13.9	8.0
	calcd.	58.1	20.0	13.9	8.0
Nd _{2.00} (OH) _{4.00} (SO ₄) _{1.01} ·2.20H ₂ O	obsd.	58.1	19.5	13.7	8.0
	calcd.	58.5	19.7	13.8	8.0
Sm _{2.00} (OH) _{4.00} (SO ₄) _{1.01} ·2.04H ₂ O	obsd.	59.7	19.3	13.5	7.3
	calcd.	59.9	19.3	13.5	7.3
Eu _{2.00} (OH) _{3.98} (SO ₄) _{1.00} ·2.10H ₂ O	obsd.	59.6	19.2	13.2	7.5
	calcd.	60.1	19.0	13.4	7.5
Gd _{2.00} (OH) _{3.98} (SO ₄) _{1.00} ·2.16H ₂ O	obsd.	60.5	18.5	13.0	7.5
	calcd.	60.8	18.6	13.1	7.5

Tb³⁺ cations, connecting the polyhedra to construct the host layer parallel to the *a*- and *c*-axes. A typical *m* = 2 compound reported is RE(OH)₂NO₃·H₂O,^{1a} in which NO₃ ions participate in the coordination to lanthanide ions. One of the most striking differences is that NO₃ ions are coordinated to the lanthanide ions in one host layer, while the sulfate group bonds to two Tb cations in adjacent layers, linking them in a *trans*-bidentate configuration. This unique structure is induced by sulfate groups with two negative charges. In this regard, the present Tb-hydroxysulfate compound can be regarded as a kind of pillared material as well as a new family of LREHs. Efforts to exchange the sulfate with other anionic species even under hydrothermal conditions failed. This result is compatible with the pillared structure.

Extended Synthesis of Layered Rare-Earth Hydroxysulfates. Layered rare-earth hydroxysulfate series can be extended to light lanthanide members with larger cationic radius, from Pr to Tb. The results of elemental analysis, listed in Table 1, confirm a general chemical formula of Ln₂(OH)₄SO₄·*n*H₂O (Ln = Pr to Tb, *n* ~ 2). XRD patterns (Supporting Information, Figure S2) also confirm the isostructural orthorhombic structure for these compounds. The in-plane parameters, both *a* and *c*, decreased linearly according to the atomic number of Ln, which can be ascribed to lanthanide contraction (Figure 7). On the other hand, the basal spacing was nearly invariable

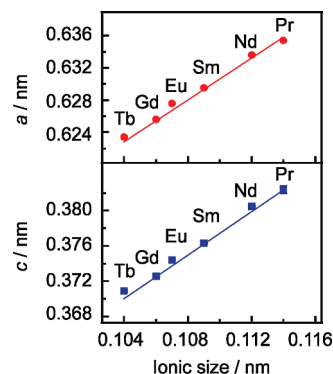


Figure 7. Correlation of in-plane lattice parameters, *a* and *c*, with the rare-earth cation size. Some standard derivations are too small to be distinguished in the figure. The cation size of nine-coordinated rare-earth cations are cited from ref 18 by Shannon.

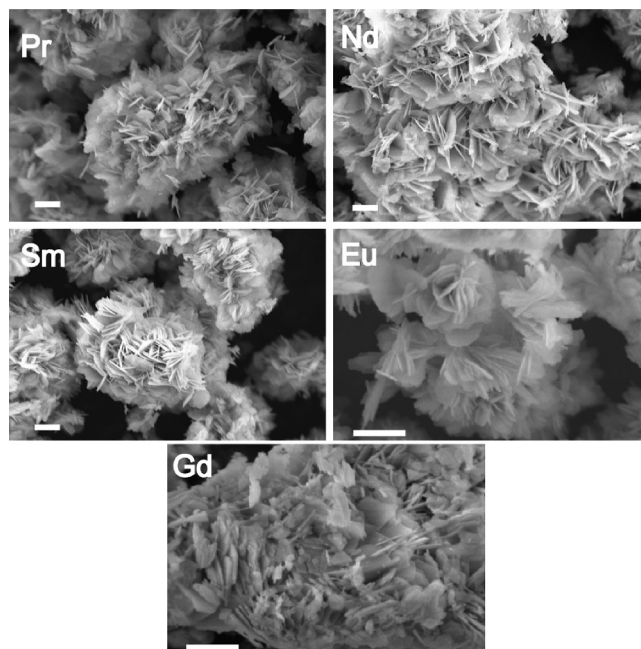


Figure 8. SEM images of layered rare-earth hydroxysulfates from Pr to Gd. Scale bar is 2 μ m.

between 0.830 nm (Tb sample) and 0.840 nm (Pr sample), consistent with the rigid pillared structure. SEM observations (Figure 8) revealed that as-prepared samples comprised aggregates of thin flakes. TEM images of Sm sample showed that thin flakes were grown in a hexagonal shape with well-developed edges.

Figure 9 shows FT-IR spectra of obtained layered rare-earth hydroxysulfates. Some characteristic modes, such as the hydrogen bonding-free O-H stretching mode and triple splitting ν_3 mode of the sulfate groups, shifted progressively depending on lanthanide cations, suggesting stronger interaction between hydroxyl groups and sulfate groups to lanthanide cations of smaller cationic radius.² In addition, the ν_3 mode became obviously asymmetric for Pr sample, implying the higher distortion of sulfate groups.^{12d}

The bonding of hydroxyl groups to lanthanide cations can also be explored through their thermal decomposition behavior. The compounds underwent a similar two-step

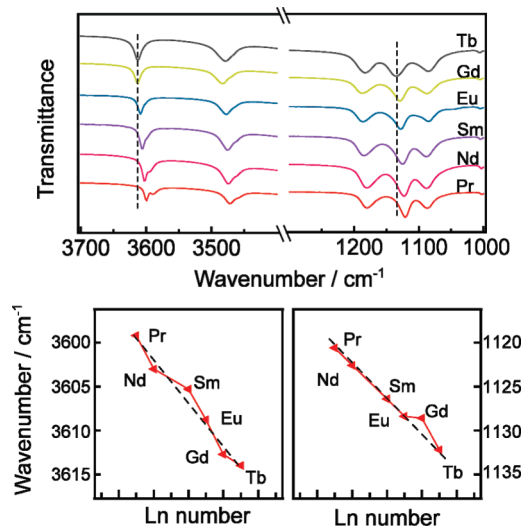


Figure 9. FT-IR spectra of layered rare-earth hydroxysulfates with the depiction of absorption peaks around 3600 and 1100 cm^{-1} .

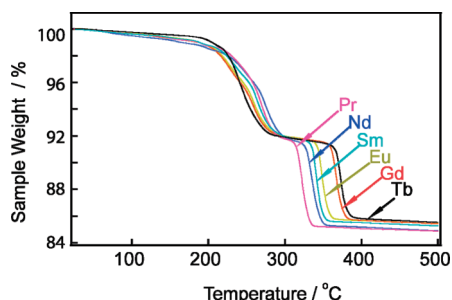


Figure 10. TG profiles of layered rare-earth hydroxysulfates.

weight loss in the TG curves (Figure 10), corresponding to the removal of water molecules and dehydroxylation of the host layers. The second dehydroxylation reaction, involving the breaking of $\text{Ln}^{3+}-\text{OH}^-$ bonding, proceeded at higher temperature from the Pr to Tb samples. This trend of higher stability in hydroxide layers for smaller lanthanides is consistent with the observation made from FT-IR data and the evolution of cell parameters above.

Photoluminescence Properties. The present layered $\text{Ln}_2(\text{OH})_4\text{SO}_4 \cdot n\text{H}_2\text{O}$ compounds showed PL properties, as exemplified by Eu and Tb cases described below. For the Eu sample, the room-temperature excitation spectrum monitored within the $^5\text{D}_0-^7\text{F}_2$ line at 617 nm displayed a series of sharp lines ascribable to intra- $4f^6$ transitions within the $\text{Eu}^{3+} 4f^6$ electronic configurations (Figure 11).^{19a} The high and broad band below 270 nm is generated from the charge transfer between O^{2-} and Eu^{3+} , which has been observed for Eu^{3+} doped YVO_3 ^{19a} and $(\text{Eu}_{1-x}\text{Gd}_x)_2\text{O}_3$.^{8b} The emission spectrum consists of typical $^5\text{D}_0-^7\text{F}_J$ ($J = 0-4$) transitions at 580.6, 589.4, 617.6, 652.2, and 697.8 nm, respectively. The splitting of these $^5\text{D}_0-^7\text{F}_J$ lines suggests that Eu^{3+} ions occupy a noninversion site in the structure. In addition, the prominent $^5\text{D}_0-^7\text{F}_2$ line (617.6 nm) was slightly red-shifted compared to the anion-exchangeable $m = 1$ phases such as

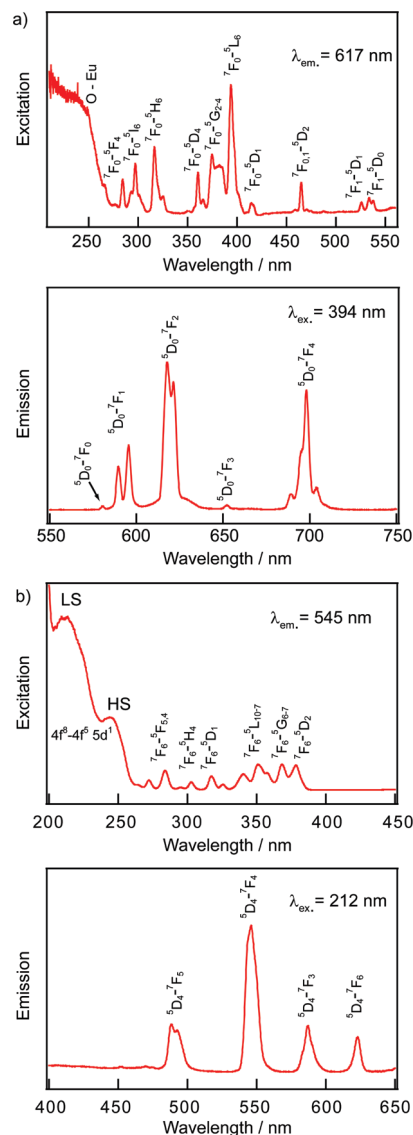


Figure 11. Room-temperature excitation and emission spectra of (a) layered Eu-hydroxysulfate and (b) layered Tb-hydroxysulfate.

$\text{Eu}(\text{OH})_{2.5}\text{Cl}_{0.5} \cdot n\text{H}_2\text{O}$ and $\text{Eu}(\text{OH})_{2.5}(\text{NO}_3)_{0.5} \cdot n\text{H}_2\text{O}$ (both at 612 nm).^{5a,c} Note that anions such as Cl^- and NO_3^- in the above compounds do not participate in the coordination of Eu^{3+} ions. Incorporation of sulfate to the coordination sphere may be responsible for the shift.

The Tb-hydroxysulfate compound also exhibited distinct PL features. In the excitation spectrum, strong spin-allowed (low-spin, LS) and spin-forbidden (high-spin, HS) inter-configurational $\text{Tb}^{3+} 4f-5d$ transition bands were observed.^{19b} The LS transition band was much stronger than the HS bands, greatly different from that in the $m = 1$ phases $\text{Tb}(\text{OH})_{2.5}\text{Cl}_{0.5} \cdot n\text{H}_2\text{O}$ and $\text{Tb}(\text{OH})_{2.5}(\text{NO}_3)_{0.5} \cdot n\text{H}_2\text{O}$.^{5b,c} A sharp green emission of 545 nm for Tb^{3+} was observed under UV excitation at 212 nm.

Conclusions

We have successfully synthesized a new family of layered rare-earth hydroxysulfates with a general formula of $\text{Ln}_2(\text{OH})_4\text{SO}_4 \cdot n\text{H}_2\text{O}$ ($\text{Ln} = \text{Pr to Tb}$; $n \sim 2$). Various characterizations including XRD, TG-DTA, and FT-IR

(19) (a) van Pieterse, L.; Reid, M. F.; Wegh, R. T.; Sovarna, S.; Meijerink, A. *Phys. Rev. B* **2002**, *65*, 045113. (b) van Pieterse, L.; Reid, M. F.; Burdick, G. W.; Meijerink, A. *Phys. Rev. B* **2002**, *65*, 045114.

measurements provide convincing proof that sulfate groups bridge the host layers through direct coordination to lanthanide cations. As-prepared layered rare-earth hydroxy-sulfate can transform into layered rare-earth oxysulfates ($\text{Ln}_2\text{O}_2\text{SO}_4$) by a simple thermal-induced dehydroxylation process (up to 450 °C), providing an environmentally clean and convenient route to produce this important material capable of large volume oxygen storage. Eu and Tb samples exhibited PL properties with characteristic red and green emissions, respectively.

Acknowledgment. This work was supported by the World Premier International Research Center (WPI) Initiative on

Materials Nanoarchitectonics, MEXT, Japan, and CREST of the Japan Science and Technology Agency (JST).

Supporting Information Available: Table list of the data for Kissinger's plot, SEM image of $\text{Tb}_2\text{O}_2\text{SO}_4$ after heating Tb sample at 1000 °C, XRD patterns of layered rare-earth hydroxides from Pr to Tb, and XRD patterns of layered rare-earth oxysulfate compounds (PDF). This material is available free of charge via the Internet at <http://pubs.acs.org>.

Note Added after ASAP Publication. There was an error in the numbering of the figures in the Results and Discussion section in the version published ASAP October 14, 2010; the corrected version was published ASAP November 2, 2010.